

X-ray Emission Diagnostics from the M87 Jet

E. S. Perlman^a A. S. Wilson^b

^aJoint Center for Astrophysics, University of Maryland, Baltimore County

^bAstronomy Department, University of Maryland, College Park

We use Chandra, HST and VLA observations of M87 to investigate the physics of X-ray emission from AGN jets. We find that X-ray hotspots in the M87 jet occur primarily in regions with hard optical-to-X-ray spectra and lower than average polarization. Particle injection appears to be required both continuously in the jet sheath as well as locally at X-ray hotspots.

1. Introduction and Observations

The M87 jet is the nearest (16 Mpc, giving a scale of $1'' = 78$ pc) and highest surface-brightness jet in the optical, radio and X-rays. As such it makes an excellent prototype for studying jet physics. The jet shows only modest differences in morphology between the optical and radio: in the optical the jet appears knottier and is more concentrated along the centerline (Sparks, Biretta & Macchetto 1996). Baade (1956) showed that its radio-optical emission was synchrotron radiation, on the basis of its high polarization. X-ray emission from the jet of M87 was first cleanly separated from Virgo cluster X-ray emission by *Einstein* (Biretta, Stern & Harris 1991), but until the launch of *Chandra*, there was essentially no information on its X-ray morphology.

Deep Chandra observations (Wilson & Yang 2002) of M87 were taken 2000 July 29-30 with ACIS-S. We compare those data to HST observations (Perlman et al. 2001) taken 1998 February and April, which include 7 bands between 0.3-2.05 μm wavelength, and to HST (V band) and radio (15 GHz) polarimetry observations (Perlman et al. 1999), which were obtained in 1995 May and 1994 February respectively. We convolved the HST and VLA images with Gaussians to a common resolution of $0.5''$ (FWHM) for morphology comparisons; however, we have chosen to leave the polarimetry data at full ($0.2''$) resolution to bring out relevant details.

We show in Figure 1 the image of the jet in the

0.3-1.5 keV band (where the PSF is smallest in size and varies the least), after maximum-entropy deconvolution using a monochromatic 1 keV PSF. Deconvolution of the *Chandra* data improved the resolution from $0.84''$ to $0.54''$ (FWHM), enabling us to resolve knot HST-1 from the nucleus and better separate other features. Superposed as contours on this are (at left) an HST I-band image of the jet, Gaussian smoothed to $0.5''$ resolution, and (at right) an unsmoothed HST polarization image ($0.2''$ resolution). In Figure 2 we show the run of X-ray flux, along with softness ratios $\text{SR1} = F(0.3-1 \text{ keV})/F(1-3 \text{ keV})$ and $\text{SR2} = F(1-3 \text{ keV})/F(3-10 \text{ keV})$ as well as α_{ox} , the optical-to-X-ray spectral index.

A full accounting of our work will appear as Perlman & Wilson (2003). We refer the reader to that paper for details on our data reduction and deconvolution procedures. Here we summarize some of the findings, particularly as respects the issue of particle acceleration.

2. Jet Morphology, Spectrum and Polarimetry

The optical and X-ray emission of the jet (Figure 1) track fairly closely in most regions; however, some significant differences are seen. In particular, two bright X-ray hotspots are located where there is no corresponding optical hotspot: in the interknot region between knots D and E, and in the interknot region between knots C and G (both were mentioned in Marshall et al. 2002

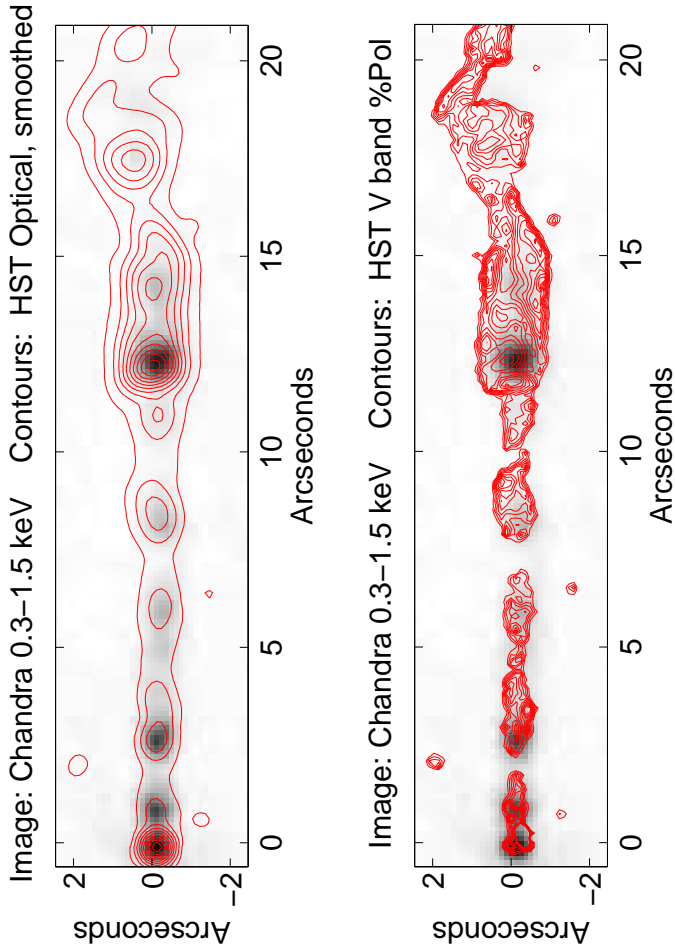


Figure 1. *Left panel.* Deconvolved *Chandra* 0.3–1.5 keV image of the jet with contours from a smoothed *HST*I-band (F814W) optical image. In both cases, the scaling is by the square root of image values. *Right panel.* Deconvolved *Chandra* 0.3–1.5 keV image of the jet with contours from a full-resolution *HST* optical polarimetry image. The greyscaling is identical to the above; however, the contours begin at 5% polarization and go up to 60%.

and Wilson & Yang 2002). In addition, the X-ray maxima of a two knots (E and F) are located a few tenths of an arcsecond upstream of their optical maxima.

All components are consistent with an X-ray spectral index $\alpha_x = 1.3$. This has been reported before for other components by Wilson & Yang and Marshall et al.; however, our analysis is the first to isolate knot HST-1 (see also later) as well as an attempt to fit a spectral index map (not shown). There do, however, appear to be variations in the softness ratios (Figure 2), which decrease significantly at distances $< 4''$ from the nucleus. The variations in SR1 are consistent with a gradually increasing column in the innermost 300 pc of the jet. Significant improvements in the spectral fits are obtained with columns $N(H) = 8.7 \times 10^{20} \text{cm}^{-2}$ for the nucleus (previously noted by Wilson & Yang) and $6.5 \times 10^{20} \text{cm}^{-2}$ for HST-1. The variations in SR2, however, cannot be explained by an increasing column at these moderate $N(H)$ values. Rather, they suggest a hardening of the jet spectrum at high energies, but there are too few photons in the hard band to adequately constrain this.

There is considerably more variation in α_{ox} than in α_x . Knot HST-1 has a much harder optical-to-X-ray spectrum than any other knot, with $\alpha_{ox} = 0.9$. The remainder of the inner jet has $\alpha_{ox} = 1.2–1.5$, with steeper spectra at larger distances from the nucleus. In addition to this pattern, one also sees small flattenings at the positions of the X-ray hotspots. The additional flattenings are suggestive of localized particle acceleration at the knot maxima (see §3). The jet’s optical-to-X-ray spectrum becomes even steeper beyond knot A (12.4'' from the nucleus), reaching $\alpha_{ox} = 1.8$ in knot C. Interestingly, the knot A-B-C complex does not show significant spectral hardening near the knot maxima.

X-ray flux is strongly anti-correlated with optical polarization (Figure 1), although the details of the relationship differ in the inner and outer jet. In all the knots in the inner jet, the X-ray flux peak is located at a local polarization minimum with $P < 20\%$, similar to the optical flux-optical polarization anti-correlation noted in Perlman et al. (1999). Immediately upstream from inner

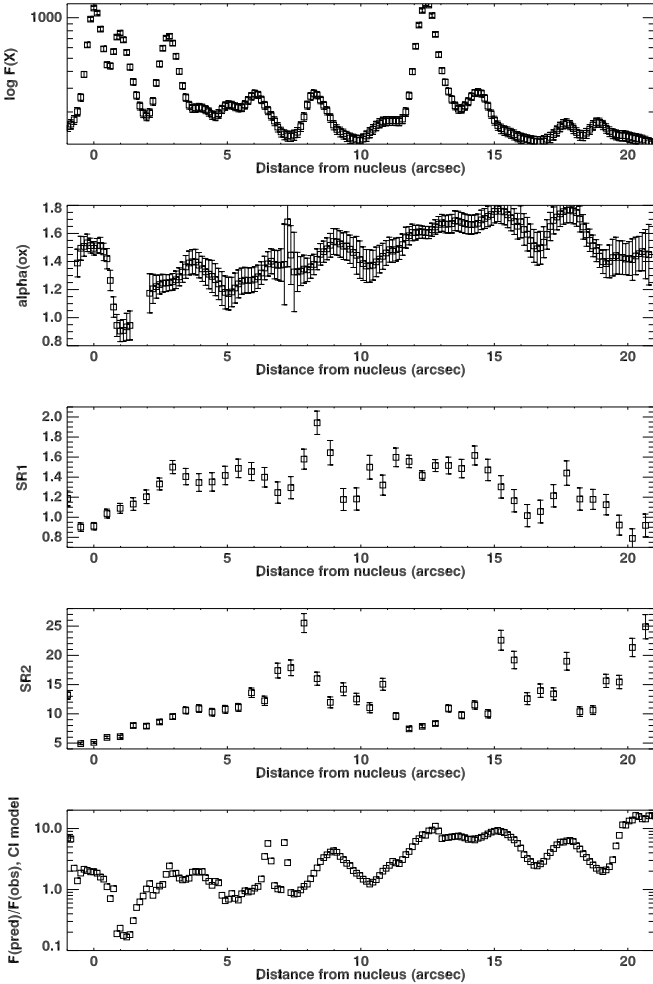


Figure 2. *Top Panel.* The run of X-ray flux in the deconvolved *Chandra* image. Plotted against this (with the same distance scale) are: *Second from top.* Optical-to-X-ray spectral index, *Third and Fourth from the top.* Softness ratios SR1 and SR2, and *Bottom.* The comparison of predicted to observed 1 keV flux from the continuous injection synchrotron model.

jet knot maxima we see increases in polarization and magnetic fields to the jet, while downstream from the knot maxima we see increased polarization but magnetic fields parallel to the jet. In the outer jet, the anti-correlation between X-ray flux and optical polarization is weaker. Knot A's maximum is located at a local minimum in polarization although unlike the inner jet knots the polarization there is still appreciable (35%) rather than consistent with zero. The peak of knot B is also located in relatively low polarization regions, but there are also polarization minima in the knot A-B-C complex which do not correspond to X-ray maxima. In addition, the X-ray peak of knot C is located in a fairly high polarization region.

3. Physical Implications

X-ray synchrotron emitting particles have lifetimes of only a few to tens of years assuming near-equipartition magnetic fields (e.g., Meisenheimer, Röser & Schlötelburg 1996, Heinz & Begelman 1997), meaning that in situ particle acceleration is required to produce the observed X-ray emission extending over a jet 7000 ly long. Can we identify loci of particle acceleration? In Figure 2 one notices an excellent correlation (at least in the inner jet) between the loci of X-ray flux maxima and the loci of flat optical-to-X-ray spectrum regions. Such spectral changes are suggestive of local particle acceleration in the knot maxima. However our modeling shows that to be insufficient to explain the observed X-ray emission.

We fit the radio to optical data with synchrotron spectrum models, and then use the models to predict the X-ray flux and spectral index in each pixel. We have done this using the code of Leahy (1991) and Carilli et al. (1991). Three models were fit: (1) the Jaffe & Perola (1972) model, which assumes no continuous particle injection and but includes pitch-angle re-isotropization; (2) the Kardashev (1962) and Pacholczyk (1970) model, which assumes neither particle injection nor pitch-angle scattering; and (3) a continuous injection (CI: Heavens & Meisenheimer 1987) model, under which a power law distribution of electrons is continuously injected. We show in the bottom panel of Figure 2 the ratio

F_{pred}/F_{obs} at 1 keV for the continuous injection model. The Jaffe & Perola model is not shown because it underpredicts the X-ray flux by orders of magnitude at many places and predicts an exponential decay of the X-ray spectral index (not observed), while the Kardashev-Pacholczyk model is not shown because it consistently underpredicts the X-ray flux by large factors and predicts too steep a spectral index.

Two main patterns can be seen in this plot. In most of the jet (except for knot HST-1), $F_{pred}/F_{obs} \sim 1 - 10$, meaning that particle acceleration occurs within 100-10% of the volume of the jet. There is a gradual increase in F_{pred}/F_{obs} as the distance from the nucleus increases. Small increases in F_{pred}/F_{obs} occur at knot maxima in the inner jet. This suggests that if particle acceleration occurs within the knot maxima, as suggested by the optical-to-X-ray (this paper) and optical spectra (Perlman et al. 2001) at these points, the loci of particle acceleration must be much smaller than *Chandra* can resolve.

Knot HST-1 appears to be a special case. It is the only place in the jet where the continuous injection model significantly *underpredicts* the X-ray flux. The reason for this is unclear. Knot HST-1 is known to be very active, with superluminally moving components (Biretta et al. 1999). Recently, HST-1 has shown blazar-like X-ray 'flaring' (Harris, these proceedings). It is possible that this variability plays a part in the anomalous F_{pred}/F_{obs} seen in HST-1. Alternately, an extra emission component could be present in the jet at higher energies; however, our modeling does not have sufficient angular resolution to test this hypothesis.

Importantly, we do *not* see large departures in the value of F_{pred}/F_{obs} in inter-knot regions. Moreover, the spectral models that do not include particle injection or acceleration still underpredict the X-ray emission at these loci by large factors. Thus even in inter-knot regions we find evidence of continuous particle injection, most likely operating in the sheath of the M87 jet. A similar conclusion was reached by Jester et al. (2001) for 3C 273 on the basis of radio-optical data.

Interestingly, we see different polarization signatures in the regions where our modeling indi-

cates *in situ* particle acceleration. As shown in Figure 1 and Perlman et al. (1999), the sheath of the M87 jet exhibits high polarization and magnetic fields parallel to the jet, while the knot maxima have either low or no polarization. Thus while the knots appear to be shock-like features (Perlman et al. 1999), where Fermi acceleration may be the dominant process, a different mechanism may operate in the sheath.

REFERENCES

- [1] Baade, W., 1956, ApJ, 123, 550
- [2] Biretta, J. A., Stern, C. P., & Harris, D. E., 1991, AJ, 101, 1632
- [3] Carilli, C. L., Perley, R. A., Dreher, J. W., & Leahy, J. P., 1991, ApJ, 383, 554
- [4] Harris, D. E., these proceedings
- [5] Heavens, A., & Meisenheimer, K., 1987, MNRAS, 225, 335
- [6] Heinz, S., & Begelman, M. C., 1997, ApJ, 490, 633
- [7] Jaffe, W. J., & Perola, G. C., 1973, A&A, 26, 421
- [8] Jester, S., Röser, H.-J., Meisenheimer, K., Perley, R., Conway, R., 2001, A&A, 373, 447
- [9] Kardashev, N. S., 1962, Soviet Astronomy AJ, 6, 317
- [10] Leahy, J. P., 1991, in Beams and Jets in Astrophysics (Cambridge), p. 100]
- [11] Meisenheimer, K., Röser, H.-J., & Shlötelburg, M., 1996, A&A, 307, 61]
- [12] Perlman, E. S., Biretta, J. A., Zhou, F., Sparks, W. B., Macchetto, F. D., 1999, AJ, 117, 2185
- [13] Perlman, E. S., Biretta, J. A., Sparks, W. B., Macchetto, F. D., Leahy, J. P., 2001, ApJ, 551, 206
- [14] Sparks, W. B., Biretta, J. A., & Macchetto, F. D., 1996, ApJ, 473, 254
- [15] Wilson, A. S., & Yang, Y., 2002, ApJ, 568, 133